Ablative Stabilization of the Deceleration Phase Rayleigh-Taylor Instability

V. Lobatchev[1] and R. Betti[2]

[1]Laboratory for Laser Energetics, Department of Mechanical Engineering, University of Rochester, Rochester, New York 14623

[2]Laboratory for Laser Energetics, Departments of Mechanical Engineering and Physics and Astronomy, University of Rochester, Rochester, New York 14623

(Received 26 July 2000)

The growth rates of the deceleration-phase Rayleigh-Taylor instability for imploding inertial confinement fusion capsules are calculated and compared with the results of numerical simulations. It is found that the unstable spectrum and the growth rates are significantly reduced by the finite ablation flow at the shell's inner surface. For typical direct-drive capsules designed for the National Ignition Facility, the unstable spectrum exhibits a cutoff for $l \approx 90$.

PACS numbers: 52.35.Py, 47.20.–k, 52.40.Nk

In inertial confinement fusion (ICF) [1], a spherical shell of cryogenic deuterium and tritium (DT) filled with DT gas is accelerated by direct laser irradiation or x rays produced by a high-Z enclosure (hohlraum). The laser pulse is designed to drive multiple shocks [1–3] through the shell and to accelerate it to the implosion velocity required for ignition. The time interval corresponding to the shell acceleration is commonly referred to as the "acceleration phase." The shocks set the shell on the desired adiabat and merge into a single shock before reaching the shell's center. Such a single shock is reflected off the center and impulsively slows down the incoming shell. Additional shocks may be reflected off the shell and its center until the lower-density material enclosed by the shell (the so-called "hot spot") reaches a sufficiently large pressure to slow down the shell in a continuous (not impulsive) manner. Such a continuous slowing down of the shell up to the stagnation point occurs over a period of a few hundred picoseconds and is referred to as the continuous "deceleration phase." Figure 1 shows the time evolution of the deceleration g of a shell designed for direct-drive ignition [3] on the National Ignition Facility (NIF). The time $t = 0$ represents the stagnation point, and the continuous deceleration starts at about 200 ps before stagnation. During the deceleration phase, the hot-spot pressure, density, and temperature increase until reaching the ignition conditions determined by temperatures and areal densities exceeding 10 keV and 0.3 g/cm^2, respectively [1]. It is well known that the shell's outer surface is unstable to the Rayleigh-Taylor (RT) instability during the acceleration phase; however, because of mass ablation, the instability growth rates are significantly reduced [4]. The thickness of ICF shells is chosen to prevent the shell from breaking up when the RT bubble amplitude equals the shell thickness. Even when the shell integrity is preserved during the acceleration phase, the hot-spot ignition can be quenched [5] by the deceleration-phase RT instability. The latter is the instability of the shell's inner surface that occurs when the shell is decelerated by high pressure building up inside the hot spot. The deceleration RT causes the cold shell material to penetrate and cool the hot spot, preventing it from achieving ignition conditions. Typical seeds for the deceleration-phase RT are the surface nonuniformities that feed through the shell from the outer surface during the acceleration-phase instability.

It is common wisdom that the deceleration-phase RT is classical [6] and all modes are unstable. The finite density-gradient scale length [7] reduces the instability growth rates which can be approximated by the classical fitting formula [1]

$$\gamma_{\text{dec}} \approx \sqrt{\frac{kg}{1 + kL}}, \tag{1}$$

where L is the shell's density-gradient scale length and k is the perturbation wave number approximately equal to l/R with R being the hot-spot radius and l the mode number. Observe that Eq. (1) indicates that all modes are unstable with the fastest-growing modes having short wavelengths ($kL \gg 1$) and growth rates $\gamma_{\text{dec}}(kL \gg 1) \simeq \sqrt{g/L}$. As shown in Ref. [7], the finite density gradient scale length is produced by the thermal conduction inside the hot spot.

In this Letter, we show that mass ablation from the shell's inner surface significantly reduces the deceleration RT growth rates, leading to much lower growth rates for short wavelength modes than predicted by Eq. (1) and to

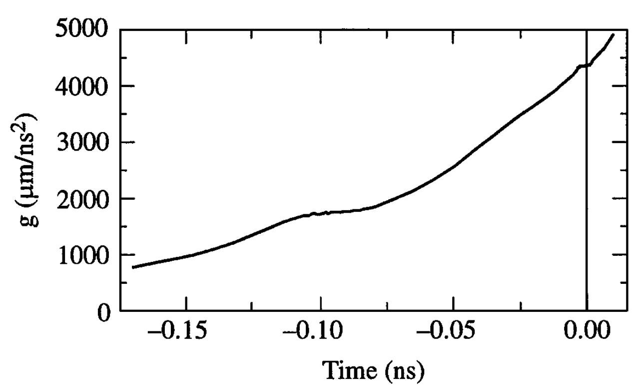

FIG. 1. Time evolution of the inner shell surface deceleration for a direct-drive NIF capsule [3]. Time $t = 0$ is the stagnation time.

a cutoff in the unstable spectrum. Mass ablation is caused by the heat flux leaving the hot spot and depositing on the shell's inner surface. We have calculated the ablation velocity and the shell's density-gradient scale length during the deceleration phase. Then, using the RT theory of Ref. [8], we have calculated the growth rates and compared them with the results of numerical simulations of an imploding direct-drive NIF-like capsule. We find that the cutoff mode number for the deceleration-phase RT is approximately $l_{\text{cutoff}} \approx 90$.

The NIF-like capsule [3] is a 345 μm thick shell of DT ice with an inner radius of 1350 μm driven by a 9.3 ns, 1.5 MJ laser pulse, which sets the shell on a $\alpha = 3$ adiabat. The shell is filled with DT gas with a density of 2×10^{-4} g/cm^3.

We have used the 1D code LILAC [9] output at 9.5 ns characterizing the beginning of the coasting phase, as the input for a high-resolution 2D Eulerian hydro code [10], solving the single-fluid mass, momentum, and energy equations, which include Spitzer conduction, local alpha deposition, and bremsstrahlung losses on a very fine grid. The high resolution is needed to correctly simulate the growth of short-wavelength modes. Aside from the bremsstrahlung losses, the code solves the same single-fluid equations on which the theory is based, providing a robust check of the theoretical results. The one-dimensional results have also been compared with the 1D code LILAC showing good agreement during the deceleration phase until the onset of the burn wave. The RT evolution is investigated by introducing a small-amplitude 2D perturbation of the hydrodynamic variables at about 200 ps before stagnation when the continuous deceleration phase begins.

The first step of the analysis concerns the calculation of the ablation velocity on the shell's inner surface surrounding the hot spot. The thermal energy escaping the hot spot via thermal conduction is absorbed by the shell material, which gains internal energy and ablates off the shell into the hot spot. The hot-spot evolution is governed by the mass, momentum, and energy conservation equations. The analysis is greatly simplified if the equations of motion are written in the Lagrangian form:

$$\frac{1}{\rho} = \frac{1}{3}\frac{\partial r^3}{\partial m}, \tag{2}$$

$$\frac{\partial U}{\partial t} + r^2 \frac{\partial P}{\partial m} = 0, \tag{3}$$

$$c_v \rho^{2/3} \frac{\partial}{\partial t} \frac{T}{\rho^{2/3}} = \frac{\partial}{\partial m} \kappa(T) r^4 \rho \frac{\partial T}{\partial m} + \frac{\rho}{4m_i^2} \theta E_\alpha \langle \sigma v \rangle, \tag{4}$$

where $c_v = 3/2A$ is the specific heat at constant volume, $A = m_i/(1+Z)$, m_i and Z are the average ion mass and atomic number, respectively ($Z = 1$ for DT), $\kappa(T) = \kappa_0 T^{5/2}$ is the Spitzer thermal conductivity, $E_\alpha =$ 3.5 MeV, θ is the absorbed-alpha-particle fraction, and $\langle \sigma v \rangle$ is the fusion reaction rate. In the simulations, the absorbed fraction is set equal to unity.

The independent variable m is proportional to the mass within the radius r

$$m = \int_0^r \rho(x,t) x^2 \, dx. \tag{5}$$

Equation (4) has been derived by using the standard ideal gas equation of state $P = \rho T/A$ and by neglecting bremsstrahlung losses which are typically smaller than the heat conduction losses. To solve the conservation equations, we adopt the subsonic flow ordering, which represents a good approximation after the shock transient. We let $t \sim R_{\text{hs}}/C_s$ (or $t \sim R_{\text{hs}}/U$), $r \sim R_{\text{hs}}$, and $U \sim \epsilon C_s$, where R_{hs} is the hot spot radius, and $\epsilon \ll 1$ represents the flow Mach number. To leading order in ϵ, Eq. (3) yields a uniform pressure so that $P \approx P(t)$. The density in the mass and energy equations can be eliminated by using the equation of state, and the fusion rate can be approximated with a quadratic power law $\langle \sigma v \rangle \approx s_\alpha T^2$ as long as $4 < T < 20$ keV. At temperatures below 4 keV, the alpha heating is smaller than the radiation losses. The energy equation can be greatly simplified by using Eq. (2) to express the radius in terms of the temperature,

$$r^3 = \frac{3}{AP(t)} \int_0^m T(m', t) \, dm', \tag{6}$$

and by defining new dependent (Ψ) and independent (η) variables as shown below:

$$\Psi = P(t)^{-2/5} \int_0^m T(t, m') \, dm' \exp\left[-D_\alpha \int_{t_0}^t P(t') \, dt'\right], \tag{7}$$

$$\eta = \eta_0 + \frac{3^{7/3}\kappa_0}{5A^{1/3}c_v} \int_{t_0}^t P(t')^{4/5} \times \exp\left[\frac{17}{6} D_\alpha \int_{t_0}^{t'} P(t'') \, dt''\right] dt', \tag{8}$$

where $D_\alpha = 0.025\theta E_\alpha s_\alpha$, η_0 is a constant, and $t = t_0$ represents the beginning of the deceleration phase. Using the new variables, a straightforward manipulation leads to the following simple form of the energy equation:

$$\frac{\partial \Psi}{\partial \eta} = \Psi^{4/3} \left(\frac{\partial \Psi}{\partial m}\right)^{3/2} \frac{\partial^2 \Psi}{\partial m^2}. \tag{9}$$

A self-similar solution of Eq. (9) can be found by setting $\Psi = a^{-21/17} F(\xi)$ and $\xi = am/\eta^{2/7}$, where ξ and $F(\xi)$ are dimensionless and a is a constant with the dimensions of $\eta^{2/7}/m$. The self-similar form of Eq. (9) is the following ordinary differential equation:

$$\frac{2}{7}\xi + F^{4/3} \left(\frac{dF}{d\xi}\right)^{1/2} \frac{d^2 F}{d\xi^2} = 0. \tag{10}$$

At the hot-spot–shell interface, the temperature is considerably less than the central hot-spot temperature. Since the temperature is proportional to $dF/d\xi$, one can neglect corrections of the order of $T_{\text{shell}}/T_{\text{hotspot}}(0,t)$ and look for a solution of Eq. (10) satisfying $dF/d\xi = 0$ at the hot-spot radius. The function F is proportional to the internal energy inside the hot spot and therefore positive by definition. The solution of such an equation can be found by numerical integration from the initial conditions $F(0) = 0$ and $F'(0) = 1$. The solution of Eq. (10) is shown in Fig. 2 indicating that $dF/d\xi$ (and therefore T) vanishes at $\xi_0 = 1.23$ and $F(\xi_0) = 0.70$. Defining the hot spot as the region with $\xi \le \xi_0$ leads to the following expression of the hot-spot mass:

$$M_{\text{hs}} = 4\pi m_{\text{hs}} = 4\pi \xi_0 \eta^{2/7}/a\,. \tag{11}$$

The constants a and η_0 [see Eq. (8)] can be determined from the initial conditions at the beginning of the deceleration phase $t = t_0$ by using Eqs. (6), (7), and (11). The ablation velocity at the shell's inner surface follows by noticing that the mass ablation rate off the shell $\dot{M}_a$ must equal the rate of change of the hot-spot mass $\dot{M}_{\text{hs}}$. Given the hot-spot radius R_{hs} and the shell density ρ_{shell}, the ablation rate is $\dot{M}_a = 4\pi R_{\text{hs}}^2 \rho_{\text{shell}} V_a$, where V_a is the ablation velocity. Thus setting $\dot{M}_a = \dot{M}_{\text{hs}}$ yields the ablation velocity

$$V_a = \frac{\dot{M}_{\text{hs}}}{4\pi R_{\text{hs}}^2 \rho_{\text{shell}}}\,, \tag{12}$$

where $\dot{M}_{\text{hs}}$ can be determined from Eq. (11). Then, using the m derivative of Eq. (7) to relate T and η, the ablation velocity can be written in terms of standard hot-spot and shell parameters:

$$V_a = \frac{12}{35}\,\frac{\xi_0}{F'(0)^{5/2}F(\xi_0)^{1/3}}\,\frac{A\kappa_0 T_{\text{hs}}(0,t)^{5/2}}{\rho_{\text{shell}}(t) R_{\text{hs}}(t)}\,, \tag{13}$$

where both the central hot-spot temperature and radius depend only on the hot-spot pressure. Using $F'(0) = 1$, $\xi_0 = 1.23$, $F(\xi_0) = 0.70$, and standard ICF units, the ablation velocity can be written in the following simple form:

$$V_a(\mu\text{m/ns}) = 6 \times 10^3\,\frac{(T_{\text{keV}}^{\text{hs}})^{5/2}}{R_{\mu\text{m}}^{\text{hs}} \rho_{\text{g/cm}^3}^{\text{shell}} \Lambda^{\text{hs}}}\,, \tag{14}$$

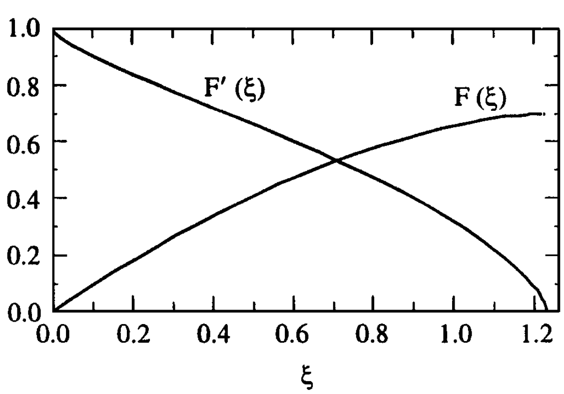

FIG. 2. Functions $F(\xi)$ and $F'(\xi)$ obtained from the numerical solution of Eq. (10).

where R^{hs}, T^{hs}, and Λ^{hs} are the hot-spot radius, central temperature, and Coulomb logarithm, and ρ^{shell} is the shell's density. Figure 3 shows the temporal evolution of the ablation velocity for the direct-drive NIF capsule under consideration obtained from Eq. (14) and calculated directly in the code using $\Lambda^{\text{hs}} = 5$. In the simulations, the ablation velocity is defined as the difference between the hydro and the hot-spot radius velocity near the shell peak density. Using the continuity of mass flow at the point r_ϕ on the shell's inner surface where the density is ϕ times the peak density, one finds $V_a^{\text{code}} = \phi[u(r_\phi) - \dot{r}_\phi]$. Such a definition of the ablation velocity (which is exact for a sharp interface with a large density jump) is almost independent of ϕ and represents a good approximation as long as the density profile is steep at the shell's inner surface.

In addition to the ablative stabilization, the RT growth rates are reduced by the well known finite density-gradient effects. Since the ablative flow at the shell's inner surface is subsonic, the minimum density-gradient scale length can be estimated using the isobaric model [11] result $L_m = 3.2A\kappa_0 T_{\text{shell}}^{5/2}/\rho^{\text{shell}} V_a$, which combined with Eq. (13) yields

$$L_m = 6.8 R_{\text{hs}}[AP(t)/\rho_{\text{shell}} T_{\text{hs}}(0,t)]^{5/2}, \tag{15}$$

where $P(t)$ is the hot-spot pressure. Following the isobaric model, the term $AP(t)/\rho_{\text{shell}}$ in Eq. (15) represents the shell temperature at its inner surface. Figure 4 shows the temporal evolution of L_m calculated from Eq. (15) and directly from the simulations.

The growth of large l modes can be determined using the planar results of Ref. [8] derived for the acceleration-phase RT. The ablative RT theory of Ref. [8] can be applied as long as the peak of the shell's density is located on its (ablating) inner surface. This occurs starting from about 150 ps before stagnation in the NIF-like capsule under consideration and $\rho_{\text{shell}} = \rho_{\text{peak}}$ should be used in Eqs. (14) and (15). Before that time, the deceleration and the growth rates are quite low, and the instability is a combination of ablative and classical RT as the peak of the density lies inside the shell at some distance

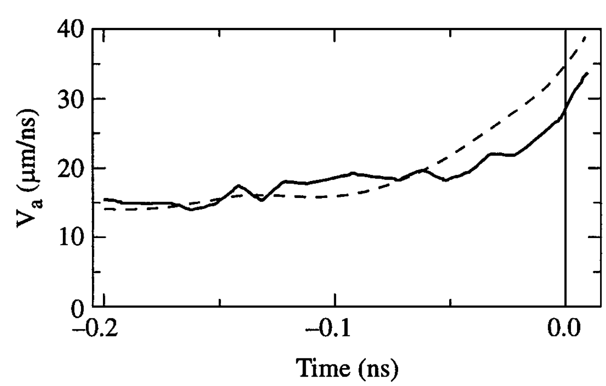

FIG. 3. Evolution of the ablation velocity at the inner shell surface of a NIF-like capsule as predicted by Eq. (14) (dashed line) and the result of numerical simulations (solid line).

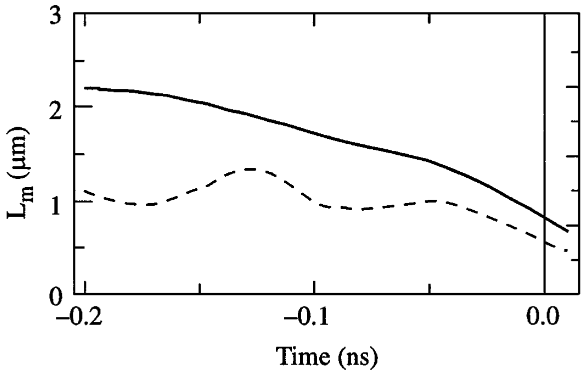

FIG. 4. Evolution of the density-gradient scale length at the inner shell surface of a NIF-like capsule as predicted by Eq. (15) (dashed line) and the result of numerical simulations (solid line).

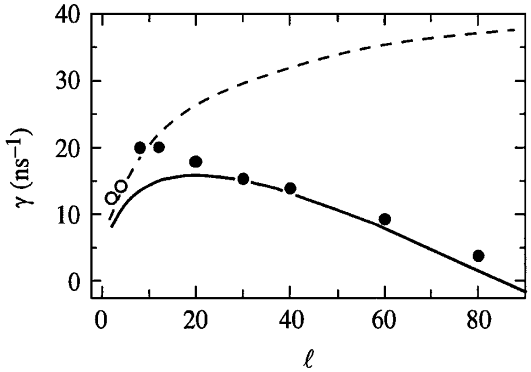

FIG. 5. Growth rate vs mode number for the deceleration-phase RT of a NIF-like capsule as predicted by Eq. (16) (solid line), Eq. (1) with $L = L_m$ (dashed line), and the results of numerical simulations (dots).

($\sim$5–15 μm) from the ablation front. More details on the RT evolution during this earlier stage will be given in a forthcoming publication. For a NIF-like capsule during the continuous deceleration phase before stagnation $\langle g \rangle \approx 3100$ μm/ns^2, $\langle V_a \rangle \approx 17$ μm/ns, $\langle L_m \rangle \approx 1.5$ μm, $R_{hs} \approx 50$–70 μm leading to a Froude number $\mathrm{Fr} \approx 0.5$, where $\mathrm{Fr} = V_a^2/gL_0$ and $L_0 = 0.12 L_m$. Using Eq. (23) and Fig. 6 of Ref. [8], we determine the appropriate growth-rate formula

$$\gamma \approx 0.9\sqrt{\frac{k\langle g \rangle}{1 + k\langle L_m \rangle}} - 1.4k\langle V_a \rangle, \tag{16}$$

where $k \simeq l/R_{hs}$ for large l's. Figure 5 compares the unstable spectrum calculated using Eq. (16) with $R_{hs} = 60$ μm, the classical RT spectrum without ablation [Eq. (1) with $L = L_m$], and the results of numerical simulations. Except for $l = 2, 4$ (open dots), the numerical growth rates are calculated in the 100-ps time interval before stagnation. The simulations of modes $l = 2, 4$ show a clear exponential growth only after the shell stagnation time, and their numerical growth rate is calculated in the 50 ps interval after stagnation. It is important to observe that the planar theory agrees well with the numerical results only for $l \geq 20$. Low l modes seem to grow faster (almost classically) than predicted by Eq. (16), indicating that convergence effects may reduce the ablative stabilization at low l. Furthermore, Fig. 5 shows that the finite ablation velocity off the shell's inner surface induces a cutoff in the RT unstable spectrum, suppressing short-wavelength modes with $l > 90$.

In conclusion, we have shown that the ablative flow off the shell's inner surface plays a crucial role in reducing the growth rate and suppressing short-wavelength modes in the deceleration-phase RT instability. We have calculated the ablation velocity and the density gradient scale length in terms of standard hot-spot parameters. Then using the theory of Ref. [8], we have determined the growth rate formula. Detailed numerical simulations have confirmed the theoretical results and have shown RT suppression at short wavelengths. If nonlocal alpha deposition is included, we expect additional stabilization after stagnation as the alpha heating of the shell's inner surface leads to a higher ablation velocity.

Part of this work was carried out when one of the authors (R. B.) was on a sabbatical leave at the CEA center in Bruyeres le Chatel (France). Special thanks to Dr. C. Cherfil and Dr. P. A. Holstein of the CEA; Dr. V. Goncharov, Dr. M. Umansky, and Dr. R. L. McCrory of LLE for many useful discussions; and Dr. M. Rosen of LLNL for suggesting the stabilizing role of ablation during the deceleration-phase RT. This work was supported by the U.S. Department of Energy under Cooperative Agreement No. DE-FC03-92SF19460.

[1] J. D. Lindl, *Inertial Confinement Fusion* (Springer, New York, 1998).
[2] T. R. Dittrich *et al.,* Phys. Plasmas **6**, 2164 (1999).
[3] LLE Review, Laboratory for Laser Energetics, University of Rochester, Rochester, NY, Vol. 79, p. 121, 1999.
[4] S. Bodner, Phys. Rev. Lett. **33**, 761 (1974); H. Takabe *et al.,* Phys. Fluids **28**, 3676 (1985); J. Sanz, Phys. Rev. Lett. **73**, 2700 (1994); R. Betti *et al.,* Phys. Plasmas **3**, 2122 (1996).
[5] R. Kishony, Ph.D. thesis, Tel Aviv University, 1999.
[6] F. Hattori, H. Takabe, and K. Mima, Phys. Fluids **29**, 1719 (1986).
[7] M. Murakami, M. Shimoide, and K. Nishihara, Phys. Plasmas **2**, 3466 (1995).
[8] R. Betti *et al.,* Phys. Plasmas **5**, 1446 (1998); V. Goncharov, Ph.D. thesis, University of Rochester, 1998.
[9] J. Delettrez and E. B. Goldman, LLE Report No. 36, 1976; also National Technical Information Service document DOE/SF/19460/118, Springfield, VA 22161.
[10] V. Lobatchev, Ph.D. thesis, University of Rochester, 2000.
[11] H. J. Kull, Phys. Fluids B **1**, 170 (1989).